AD-A166 301 EXPERIMENTAL OBSERVATION OF THE STRUCTURE OF SHOCK WAVES IN DUSTY GAS(U) FOREIGN TECHNOLOGY DIV WRIGHT-PATTERSON AFB OH H YU ET AL. 27 MAR 86 1/1

UNCLASSIFIED FTD-ID(RS)T-1262-85 F/G 20/4 NL

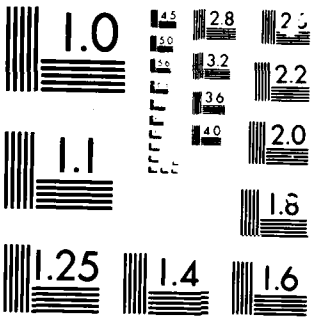

MICROCOPY RESOLUTION TEST CHART

FTD-ID(RS)T-1262-85

FOREIGN TECHNOLOGY DIVISION

EXPERIMENTAL OBSERVATION OF THE STRUCTURE OF SHOCK WAVES IN DUSTY GAS

by

Yu Hongru, Lin Jianmin, et al.

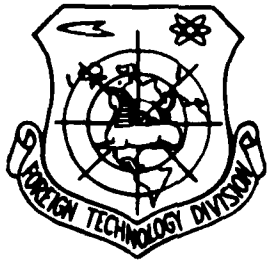

EDITED TRANSLATION

FTD-ID(RS)T-1262-85 27 March 1986

MICROFICHE NR: FTD-86-C-001673

EXPERIMENTAL OBSERVATION OF THE STRUCTURE OF SHOCK WAVES IN DUSTY GAS

By: Yu Hongru, Lin Jianmin, et al.

English pages: 13

Source: Lixue Xuebao, No. 6, 1983, pp. 531-537

Country of origin: China
Translated by: SCITRAN
F33657-84-D-0165
Requester: FTD/TQTA

PREPARED BY.

TRANSLATION DIVISION
FOREIGN TECHNOLOGY DIVISION
WP-AFB, OHIO.

GRAPHICS DISCLAIMER

All figures, graphics, tables, equations, etc. merged into this translation were extracted from the best quality copy available.

EXPERIMENTAL OBSERVATION OF THE STRUCTURE OF SHOCK WAVES IN DUSTY GAS[1]

Yu Hongru, Lin Jianmin, Yuan Shengxue, and Li Zhongfa

Institute of Mechanics, Chinese Academy of Sciences

Abstract

The structure of shock waves in dusty gas was studied by shock tube experiments. Pressure, shock wave velocity and dust concentration were measured under the condition that the dusty loading ratio was less then 0.4 and the shock Mach number was less than 1.5. The frozen and equilibrium pressures behind the shock wave can be well described by the Rankine-Hugoniot relation. But the relaxation length was significantly shorter than that calculated from the drag of a sphere at steady motion. And the disperse shock waves in dusty gas were observed. It was found that the presence of dust decreases the pressure fluctuation in the flow. The propagation velocity of the shock wave agrees with the result of the model analysis on an 'effective gas'.

This paper was recommended by editor Ling Dong Ji and was received on July 1, 1983.

1. This paper is written for the 15th anniversary of the death of our adviser Professor Guo Yong Hui.

The List of Symbols

Symbol	Definition
a	Sound velocity
$\overline{R}$	Dusty gas constant
A_p	Particle cross-section area
t	Time
C	Heat capacity of particle material
T	Gas temperature
T_p	Particle temperature
C_p	Gas heat capacity at constant pressure
u	Gas velocity
C_D	Coefficient of resistance
u_p	Particle velocity
D	Particle diameter
V	Voltage
E	Coefficient of light attenuation
x	Distance
h	Coefficient of heat conductivity
X	$=x/\beta$
I	Intensity of transmitted light
α	Sound velocity of dusty gas
k	Coefficient in formula (2)
β	$=\alpha_0\tau_0$
K	Heat conductivity
γ	Ratio of gas heat capacities
l	Thickness of particle cloud
r	Specific heat ratio of dusty gas
$\dot{m}$	Mass flux of gas
ε	$=C/C_p$
$\dot{m}_p$	Mass flux of particle cloud
ρ	Gas density
M_s	Mach number of shock wave
ρ_p	Density of dusty material
n_p	Number density of dust
σ	Concentration of dust

Nu	=hD/K Nusset number
τ_v	Velocity relaxation time
p	Pressure
μ	Coefficient of powderiness of gas
R	Gas constant
η	$=\dot{m}p/\dot{m}$

Subscript

0	Wave front or initial value
d	Dark value
f	Frozen value
c	Average value

1. Introduction

Intensive theoretical studies and numerical analysis of the structure of shock waves in dusty gas have been made by many people [1-14]. Their work was carried out with some idealized assumptions. Among them the most basic assumption was: the particles distribute uniformly in a perfect gas medium and the particle cloud was treated as continuous. For energy and momentum exchanges between the two phases, only the drag of an isolated rigid sphere at steady motion and heat conduction by convection are considered. Besides that, the results of experimental observation of the structure of shock waves of dusty gas are rare except the experiments for the measurement of the effective drag coefficient of the particle cloud.

In this paper we report the observed results of such structure of shock waves in a shock wave tube, and the driving characteristics of a dusty gas shock wave tube.

2. Description of Experiment

The shock wave tube for the experiment was installed perpendicularly with driving section in the upper position. The driving section is 1.5 meters long with an inner diameter of 84 mm; the driven section is 5 m long with an inner diameter of 185 mm. The reason for

using such big tube is to decrease the disturbance of the tube wall to the minimum. The observation area is located 4 m below the isolating diaphragm.

The dust material is aluminium oxide, with a density of 3.9-4.0 g/cm^3, and a heat capacity of 0.73 KJ/kg·K. The shape of the particles is close to sphere but the surface is not smooth. The dusty particles were jetted by attraction into the shock wave tube in the vicinity of the isolating diaphragm. The uniformity of the dusty particle distribution and the initial disturbance have important influence on the experiment. The dusty particles were jetted upwards, then the particles were reflected from the isolating diaphragm and fell down. Thus the movement of the dusty particles was basically a free fall motion and the distribution was quite uniform. Only a small amount of gas is needed for the attractive jet and the initial disturbance is very small. All the gas used in the experiment was nitrogen. The front of the shock wave was atmospheric pressure.

Besides the routine static measurement of the initial state, the propagation velocity of shock waves along the tube axis, the pressure, and the density of dusty particles were measured in the experimental process. The light attenuation method was used for the measurement of dust density. When the sizes of the particles are uniform or the size distribution is narrow, this is a simple and reliable method. We chose a low power He-Ne laser as light source. The number density of dust can be calculated according to Bouger's law by measuring the intensity of transmitted light which passed the particle cloud [13]:

$$\frac{I}{I_0} = \exp -(n, A, lE) . \qquad (1)$$

The transmitted light was measured by a photo diode. The output voltage is proportional to the intensity of incident light intensity. Therefore formula (1) can be modified to (2):

$$\sigma(t) = k \ln \frac{V_0 - V_d}{V(t) - V_d} . \qquad (2)$$

The coefficient k depends on the size and shape of dust particles, the thickness of the particle cloud and the optical loss in the optical route. We determined k value by calibration measurement of different types of dusty particles. The most serious problem in the measurement of the density of the dust density was the adsorption of particles on the observation window, which decreases the intensity of the transmitted light. When both the density and the velocity are low, the adsorption will be low. Such measurement of density in this work was used to monitor the axial uniformity of dust, and to offer the initial values of the dust density.

All the dynamic measurements were recorded by instant wave form recorders, and the data or graphs were output after the signal analysis instruments.

3. The Positive Shock Wave of Dusty Gas

If the density of dusty particles is not high, the volume occupied by the dusty particles is negligible. Then the equations of the conservations of mass, momentum, and energy are as flows:

$$\dot{m} = \rho u = \rho_0 u_0 \tag{3}$$

$$\dot{m}_p = \eta \dot{m} = \sigma u_p = \sigma_0 u_{p_0} \tag{4}$$

$$\dot{m}u + \eta \dot{m} u_p + P = (1+\eta)\dot{m}u_0 + P_0 \tag{5}$$

$$\frac{1}{2}u^2 + C_r T + \eta\left(\frac{1}{2}u_p^2 + C_r \delta T_p\right) = \frac{1}{2}u_0^2(1+\eta) + C_r(1+\eta\delta)T_0 \tag{6}$$

and plus the equation of state of ideal gas:

$$P = \rho R T . \tag{7}$$

In order to solve the seven variables of $u, \rho, T, P, u_p, \sigma$ and T_r another two equations are needed.

Generally the shock wave can be divided into three regions and disposed separately:

In the frozen region close to the wave front, because the dust density is 10^3 times higher than the gas density, and the wave front

is very thin, then the time for particles to pass through it is very short; therefore the particle velocity and temperature can be considered frozen, that is:

$$u_{pf} = u. \tag{8}$$
$$T_{pf} = T. \tag{9}$$

Substituting these two equations into equation (5) and (6), all the terms related to the dusty particles are calceled and the equations become shock wave equations of pure gas. Then the gas parameters can be obtained by solving these equations.

In the equilibrium region below the wave front, the equilibrium between the two phases is attained via the exchanges of momentum and energy; therefore we have:

$$u_{pe} = u_e \tag{10}$$
$$T_{pe} = T_e . \tag{11}$$

Substitute these equations into (5) and (6) and reorganize these equations. Then we can know that the differences from the pure gas shock wave equations are as follows: Use the equilibrium sound velocity $a_0 = \left[\frac{\Gamma}{\gamma(1+\eta)}\right]^{1/2} a_0$ to replace a_0, and use the ratio of heat capacities of dusty gas $\Gamma = (1+\eta\delta)\gamma/(1+\gamma\eta\delta)$ to replace γ. Therefore the parameters of the equilibrium region also can be obtained from the pure gas shock wave equations.

For the pressure in the frozen and equilibrium regions, the following relations exist:

$$\frac{P_f}{P_0} = \frac{2\gamma}{\gamma+1}\left(\frac{u_0}{a_0}\right)^2 - \frac{\gamma-1}{\gamma+1} \tag{12}$$
$$\frac{P_e}{P_0} = \frac{2\Gamma}{\Gamma+1}\left(\frac{u_0}{a_0}\right)^2 - \frac{\Gamma-1}{\Gamma+1} . \tag{13}$$

For the gas velocities in the frozen and equilibrium regions, the following relations exist:

$$u_f u_0 = \frac{2\gamma R}{\gamma+1} T_0 + \frac{\gamma-1}{\gamma+1} u_0^2 \tag{14}$$
$$u_e u_0 = \frac{2\Gamma \bar{R}}{\Gamma+1} T_0 + \frac{\gamma-1}{\gamma+1} u_0^2 . \tag{15}$$

Because a_0, Γ and $\bar{R}$ are always smaller than a_0, γ and R, therefore $P_c > P_1$, $u_c < u_1$. According to the equation of mass conservation, we have $\rho_c > \rho_1$. As for the temperature in these two regions, the difference is not large, and which is higher depends on the particle size and gas heat capacity.

For the two lacking equations for the solution of the relaxation region, we can use the momentum and energy exchange equations between dusty particles and gas. Because of lack of understanding of the drag of the particle cloud and heat conduction, current analytical and numerical solutions all use the drag and heat conduction of an isolated rigid sphere at steady motion:

$$\frac{du_p}{dt} = \frac{3}{4}\frac{C_p}{D}\frac{\rho}{\rho_p}(u-u_p)|u-u_p| \tag{16}$$

$$\frac{dT_p}{dt} = \frac{6KNu}{CD^2\rho_p}(T-T_p)\ . \tag{17}$$

The parameters in the relaxation region require numerical analysis. The structure of shock waves in dusty gas, according to the experimental conditions of experiment No. 201, is shown in Fig. 1.

When the coming-flow velocity $u_0=a_0$, then $M_{f1} = u_0/a_0 = 1$, and the parameters of the frozen region are same as that of the wave front. Because $a_0 < a_{0'}$ and $M_{fc} = u_c/a_0 > 1$, the parameters of equilibrium are different from that of the wave front. Under this situation, disperse shock waves without an interruption place can occur.

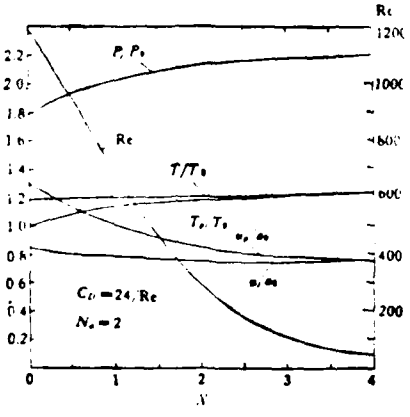

Fig. 1. Calculated shock wave structure of dusty gas. ($M_{f1} = 1.30$, $\eta = 0.17$, $D = 80\mu m$).

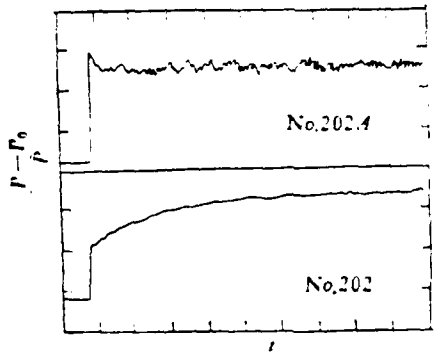

50 kpa, 0.5 ms per div

Fig. 2. Typical recorded curves of pressure. Upper: Without dust, M_s=1.44. Lower: $\eta = 0.17$, $D = 80\mu m$, $M_{f1} = 1.24$.

4. Results of Observation

As described before, the changes of shock wave velocity, pressure, and dust density were measured in the experiments. Because the dusty particles were gradually absorbed on the observation window when the shock waves propagate through it, the measured result of particle density tended to be a little higher. For the particles under free fall motion, the adsorption was not serious and the initial value of the dust density is quite accurate. We now give a discussion on the experimental data of pressure, combining the shock wave velocity and the initial dust density. The typical experimental pressure curves are shown in Fig. 2.

1. Pressure in the frozen and equilibrium regions. According to the result of analysis, the pressure in the frozen region P_f is independent of the loading ratio, size, and shape of the dusty particles. Fig. 3 is the experimental result with $\eta = 0—0.4$, $M_{sf} = 1.04—1.5$, $D = 80\mu m$ and $55\mu m$. The curve in Fig. 3 was calculated according to formula (18). From this figure we can see the experimental result verifies the theoretical prediction

$$\frac{(P_f - P_e)}{P_0} = \frac{2\gamma}{\gamma + 1}[M_{sf}^2 - 1]. \tag{18}$$

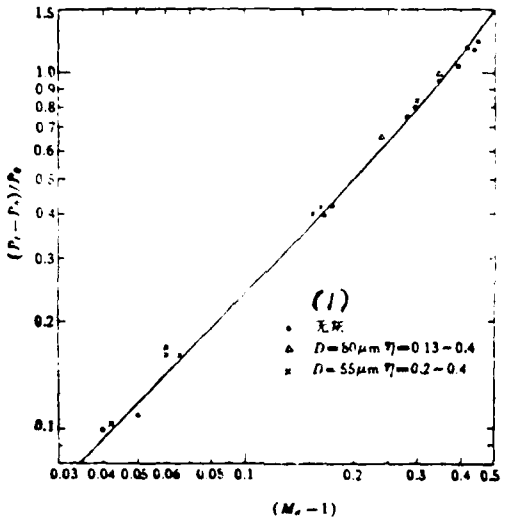

Fig. 3. The relation between the pressure of frozen region and Mach number of shock wave.
Key: (1). without dust.

The pressure in the equilibrium region is related to the loading ratio of the dusty particles. The experimental results are listed in Table 1 (all are 80μm particles).

Table 1

(1) 实验序号	$M_{s1}=\frac{u_0}{a_0}$	η	Γ	a_e/a_0	$(P_e-P_0)/P_0$		(4) 测量值/计算值
					(2) 计算值	(3) 测量值	
197	1.35	0.13	1.365	.929	1.28	1.31	1.02
201	1.30	0.17	1.356	.910	1.20	1.21	1.01
202	1.24	0.40	1.309	.817	1.48	1.35	.912

Key: (1). Serial number of experiment. (2). Calculated value. (3). Measured value. (4). Measured value/calculated value.

The calculated values listed for comparison in Table 1 were obtained according to formula (19):

$$\frac{(P_e-P_0)}{P_0}=\frac{2\Gamma}{\Gamma+1}[M_{1e}^2-1]. \qquad (19)$$

The Γ and a_0 were calculated according to the particle loading ratio η. From Table 1, the theoretical prediction agrees with the experimentally observed results. The observed results of the experiment of No. 202 are less than the calculated values, and this is due to the fact that the relaxation region is too long for a weak shock wave and the observation time is not long enough to attain the equilibrium region.

2. Characteristics of the relaxation region. The status of the relaxation region can be numerically obtained by solving equations (3-7) and (16-17). The calculated results depend on the choice of the drag coefficient and heat conductivity. Rudinger's calculation [5] shows that C_D has larger influence on the velocity and pressure than the Nusset number does. For experiments No. 197 and No. 202, in order to calculate the pressure curves (Fig. 4a) we chose Nu=2, and we chose Stokes drag and the standard drag coefficient, respectively. From this figure, we can see both curves have same tendency of change, but the relaxation length calculated with the Stokes drag formula is very long. Comparing with the experimental result (Fig. 4b), the relaxation regions of both experiments are much shorter.

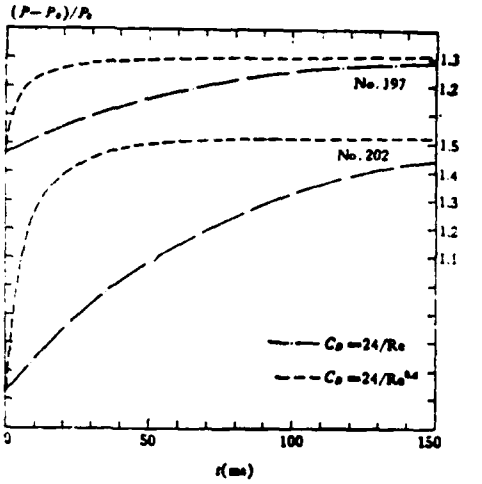

Fig. 4a. Calculated results with different resistance coefficients.

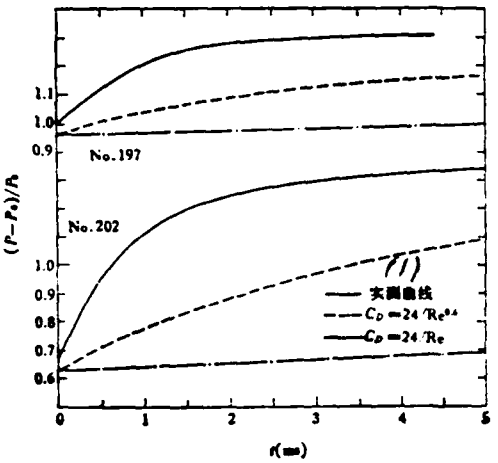

Fig. 4b. Ratios of calculated values to experimentally measured values.
Key: (1). Experimental curve.

The reason for the disagreement of calculation with Stokes drag from the experimental result is obvious: because the Reynolds number under the above condition is much larger than one. Although the standard curve of the resistance formula can represent the drag of isolated sphere steady motion, it can not reflect the influence of the disturbance of multi-particle tail flow, particle shape, surface stature, acceleration, etc. Because the measured result is far from the calculated result, the characteristics of the relatation region need further study.

3. Structure of disperse shock waves. According to the above analysis, when the propagation velocity of shock waves equals the sound velocity of the gas, disperse shock waves without interrupted wave front plane will appear. Because the intensity of the shock wave is weak and there is no interrupted plane, it is quaite difficult to generate and observe such shock waves. We recorded the pressure curve of such shock waves in the experiment of No. 219 (Fig. 5).

The condition of this experiment was as follows: driving gas pressure equals 0.54 MPa, driven gas pressure equals 0.1 MPa, dust particle diameter equals 20-30 μm, initial dust concentration equals 0.3 mg/cm^3, room temperature equals 27°C. The propagation

velocity of shock waves was obtained by comparing the output of two pressure sensors which are located a certain distance apart. The propagation velocity measured was 355 m/s.

4. The damping effect on the disturbance of dust particles. The upper curve in Fig. 2 is the pressure curve without dust and the lower curve is the pressure with dust, and all other experimental conditions were the same. We can see that the fluctuation of the upper curve is obviously larger than that of the lower curve. Usually such fluctuation is caused by turbulent flow fluctuation and the unevenness of the tube wall. The dust particles in gas have an obvious effect to depress such fluctuation.

5. Driving characteristics of dusty gas shock wave tube. Recently different studies and applications using dusty gas shock wave tubes are increasing gradually. In the design of such shock wave tubes, obtaining the required driving force is one of the main concerned problems.

Only if the propagation distance of the shock wave, that is, the distance between the shock waves and the boundary plane, is larger than relaxation length, then the pressure and velocity in the boundary plane will equal the pressure and velocity in the equilibrium region. The calculation of structural parameters of a dusty gas shock wave tube can be carried out by using the calculation formulas of the classic shock wave tube, by replacing the pure gas parameters with the thermal dynamic parameters of dusty gas.

Figure 6 gives the calculated results and experimental results of the variable cross-section shock wave tube used in our experiments. The data in this figure are the shock wave velocities in the observation region. From this figure we know the calculated results using the above model agree with the experimental results.

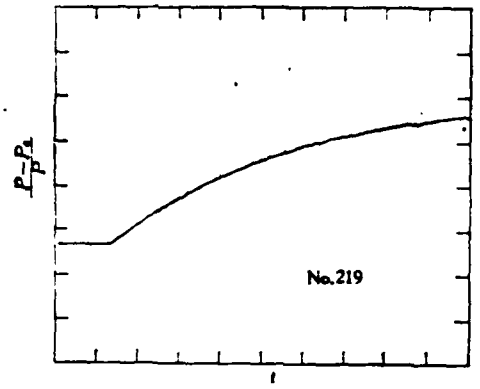

25 kpa, 0.5 ms/division

Fig. 5. Pressure curve of disperse shock wave.

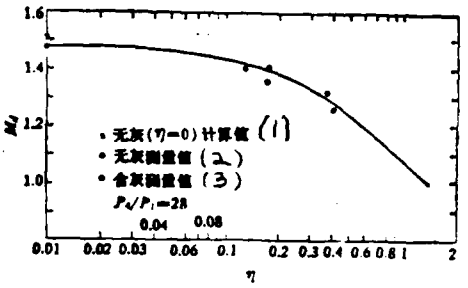

Fig. 6. Relation of particle loading ratio and shock wave Mach number.
Key: (1). Calculated values without dusty particles. (2). Measured values without dusty particles. (3). Measured values of dusty gas.

5. Conclusion

1. The parameters of the frozen and equilibrium regions can be correctly predicted by the theoretical analysis.

2. For the relaxation region, we choose the drag and heat conductivity of an isolated rigid sphere at steady motion. The tendency of change is same as that of the experimental result, but the quantitative difference if very large. Therefore further studies are needed.

3. When shock waves propagate with the sound velocity of gas in a wave front, disperse shock waves without interrupted plane were observed. This verifies the theoretical prediction.

4. The dusty particles have the disturbance effect in the damping gas flow.

5. At the location far away from the diaphragm the shock wave intensity can be predicted by using the classic shock wave formulas,

with the effective gas thermal dynamic parameters.

The authors wish to thank Mr. Li Zhongfa and Mr. Pu Yi Kang for their help in designing and building of the equipment of the experiment.

References

[1] Carrier, G. F., Shock waves in dusty gas, *Jour. of Fluid Mechanics*, 4(1958), 376.

[2] Kliegel, J. R. One dimensional flow of a gas-particle system IAS paper, 60—5 (1960).

[3] Marble, F. E., Dynamics of a gas containning small solid particles, 5th Combustion and Propulsion AGARD Coll. (1963).

[4] Kriebel, A. R., Analysis of normal shock waves in particle laden gas, *Trans. ASME, Jour. of Basic Eng.*, 86(1964), 655—665.

[5] Rudinger, G., Some properties of shock relaxation in gas flows carrying small particles, *Physics of Fluids*, 7(1964), 658—663.

[6] Lu, H. Y. & Chun, H. H., Dynamics of gas containing evaporable liquid droplets under a normal shock wave, *AIAA Jour.*, 4, 6(1966), 1008—1011.

[7] Varm, T. D. & Chopra, N. K., Analysis of normal shock waves in a gas-particle mixture, *ZAMP*, 18(1967), 650—660.

[8] Schmitt-Von Schubert, B. Shock wave structure of gas with solid particles. ZAMM, 50 (1970), 671.

[9] Narkis, Y. & Gal-or, B., Two-phase flow through normal shock, Trans. ASME, *Jour. of floid Eng.*, 971(1975).

[10] Krier, H. & Mozaffarian, A., Two-phase reactive particle flow through normal shock waves. *Int. Multiphase Flow*, 4, 1(1978), 65—79.

[11] Selberg, B. P. & Nicholls, J. A. Drag coefficient of small sphericalparticles, *AIAA Jour.*, 6 (1968).

[12] Rudinger, G., Effective drag coefficient for gas particle flow in shock tube, Trans. ASME, *Jour. of Basic Eng.* 92(1970).

[13] Hodkinson, J. R., Aerosol Sci., Ed. Davies (1966).

END

FILMED

5-86

DTIC